

Hierarchical Self-Assembly of Chiral Complementary Hydrogen-Bond Networks in Water: Reconstitution of Supramolecular Membranes

Takayoshi Kawasaki,[†] Maki Tokuhiro, Nobuo Kimizuka,* and Toyoki Kunitake[‡]

Contribution from the Department of Applied Chemistry, Faculty of Engineering, Kyushu University, Higashi-ku, Fukuoka 812-8581, Japan

Received January 3, 2001

Abstract: Spontaneous formation of complementary hydrogen-bond pairs and their hierarchical self-assembly (reconstitution) into chiral supramolecular membranes are achieved in water by mixing amphiphilic pairs of glutamate-derived melamine **6** and ammonium-derivatized azobenzene cyanuric acid **4**. Electron microscopy is used to observe formation of helical superstructures, which are distinct from the aggregate structures observed for each of the single components in water. In addition, a spectral blue-shift and induced circular dichroism (ICD) with exciton coupling are observed for the π - π^* absorption of the azobenzene chromophores. These observations are consistent with the reconstitution of the hydrogen-bond-mediated supramolecular membrane **6**–**4**. Spectral titration experiments indicate the stoichiometric integration of the complementary subunits with an association constant of $1.13 \times 10^5 \text{ M}^{-1}$. This value is considerably larger than those reported for the artificial hydrogen-bonding complexes in aqueous media. The remarkable reconstitution efficiency is ascribed to the hydrophobically driven self-organization of the amphiphilic, linear hydrogen-bond networks in water. Molecular structure of the complementary subunits plays an important role in the complexation process since it is restricted by the photoisomerized *cis*-azobenzene subunit. On the other hand, thermally regenerated *trans*-isomer **4** undergoes facile complexation with the counterpart **6**. The present reconstitution of supramolecular membranes provides the first example of complementary hydrogen-bond-directed formation of soluble, mesoscopic supramolecular assemblies in water.

Introduction

Biological supramolecular assemblies as exemplified by nucleic acid multiplexes, multimeric proteins, nucleic acid–protein complexes, and viruses provide a variety of chiral superstructures in the mesoscopic range (ca. 10–1000 nm in scale).¹ They spontaneously self-assemble in aqueous media by ingeniously employing multiple noncovalent interactions—such as electrostatic interactions, hydrogen bonding, dipole–dipole interactions, and hydrophobic association. Inspired by these biological self-assemblies, construction of supramolecular aggregates has been an area of active research.² Especially, multiple hydrogen bonds between complementary molecular components are popularly used as driving force for the formation of dimers or oligomeric aggregates in organic media.^{3,4} Comple-

mentary hydrogen-bond pairs are also formed in organic gels,⁵ liquid crystals,⁶ and in molecular cocrystals.⁷ Especially, the pair of melamine and cyanuric acid (or barbituric acid) has been popularly used to create a variety of supramolecular motifs—such as linear tapes, crinkled tapes, and circular structures.^{7e,f} These architectures are mostly governed by the steric interactions among substituents introduced in the component molecules. However, formation of hydrogen-bond-directed assemblies has been largely carried out in the nonaqueous media, due to the highly deteriorating action of water molecules against hydrogen bonding.

Generally, enthalpic gain by the formation of hydrogen bonds in water is canceled by the enthalpy to break hydrogen bonds which have been formed between these molecules and water.⁸ Therefore, hydrogen bonding in the aqueous media requires integration of the other noncovalent interactions—such as hydrophobic interactions or aromatic stacking—to compensate for the entropic disadvantage. Previous efforts made for the

* Corresponding author. E-mail: kimitcm@mbox.nc.kyushu-u.ac.jp.

[†] Current address: Graduate School of Bioscience and Biotechnology, Tokyo Institute of Technology, Nagatsuda 4259, Midori-ku, Yokohama, 226-8501, Japan.

[‡] Current address: Frontier Research System, RIKEN, Wako, Saitama, 351-0198, Japan.

(1) Klug, A. *Angew. Chem., Int. Ed. Engl.* **1983**, *22*, 565.

(2) *Comprehensive Supramolecular Chemistry*; Sauvage, J.-P., Hosseini, M. W., Eds.; Pergamon: UK, 1996; Vol. 9.

(3) (a) Rebek, J., Jr. *Angew. Chem., Int. Ed. Engl.* **1990**, *29*, 245. (b) Lehn, J.-M. *Angew. Chem., Int. Ed. Engl.* **1990**, *29*, 1304. (c) Whitesides, G. M.; Mathias, J. P.; Seto, C. T. *Science* **1991**, *254*, 1312. (d) Lawrence, D. S.; Jiang, T.; Levett, M. *Chem. Rev.* **1995**, *95*, 2229.

(4) (a) Zimmerman, S. C.; Duerr, B. F. *J. Org. Chem.* **1992**, *57*, 2215. (b) Mathias, J. P.; Seto, C. T.; Simanek, E. E.; Whitesides, G. M. *J. Am. Chem. Soc.* **1994**, *116*, 1725. (c) Yang, J.; Marendaz, J.-L.; Geib, S. J.; Hamilton, A. D. *Tetrahedron Lett.* **1994**, *22*, 3665. (d) Zimmerman, S. C.; Zeng, F.; Reichert, D. E. C.; Kolotuchin, S. V. *Science* **1996**, *271*, 1095. (e) Drain, C. M.; Russell, K. C.; Lehn, J.-M. *J. Chem. Soc., Chem. Commun.* **1996**, 337.

(5) Hanabusa, K.; Miki, T.; Tagushi, Y.; Koyama, T.; Shirai, H. *J. Chem. Soc., Chem. Commun.* **1993**, 1382.

(6) (a) Mariani, P.; Mazabard, C.; Garbesi, A.; Spada, G. P. *J. Am. Chem. Soc.* **1989**, *111*, 6369. (b) Lehn, J.-M. *Makromol. Symp.* **1993**, *69*, 1. (c) Kotera, M.; Lehn, J.-M.; Vigneron, J.-P. *J. Chem. Soc., Chem. Commun.* **1994**, 197. (d) Suárez, M.; Lehn, J.-M.; Zimmerman, S. C.; Skoulios, A.; Heinrich, B. *J. Am. Chem. Soc.* **1998**, *120*, 9526.

(7) (a) Voet, D.; *J. Am. Chem. Soc.* **1972**, *94*, 8213. (b) Shimizu, N.; Nishigaki, S. *Acta Crystallogr.* **1982**, *B38*, 2309. (c) Etter, M. C. *Acc. Chem. Res.* **1990**, *23*, 120. (d) Lehn, J.-M.; Mascal, M.; DeCian, A.; Fischer, J. *J. Chem. Soc., Chem. Commun.* **1990**, 479. (e) G-Tellado, F.; Geib, S. J.; Goswami, S.; Hamilton, A. D. *J. Am. Chem. Soc.* **1991**, *113*, 9265. (f) MacDonald, J. C.; Whitesides, G. M. *Chem. Rev.* **1994**, *94*, 2383.

(8) (a) Doig, A. J.; Williams, D. H. *J. Am. Chem. Soc.* **1992**, *114*, 338. (b) Searle, M. S.; Williams, D. H.; Gerhard, U. *J. Am. Chem. Soc.* **1992**, *114*, 10697.

complementary hydrogen bonding in water took advantage of hydrophobic microenvironments which were provided by aromatic surfaces⁹ or by the interior of aqueous micelles.¹⁰ Hydrophobic interactions also played a pivotal role in the self-association of ureidotriazine derivatives in water.¹¹ On the other hand, recent studies at the air–water interface showed that the complementary hydrogen bonding is drastically facilitated, compared to that observed at the surface of aqueous micelles or bilayers.^{12–14} However to date, in situ formation of complementary hydrogen-bond pairs in water and their hierarchical self-assembly into the soluble, mesoscopic supermolecules have not been realized, despite the omnipresent examples and their significance in biology.

We have previously reported that the suitably designed amphiphilic hydrogen-bond networks form supramolecular nano-assemblies in aqueous¹⁵ as well as in organic media.¹⁶ In the aqueous system, preformed hydrogen-bond pairs of quaternary ammonium-derivatized cyanuric acids (hydrophilic subunits) and alkylated melamines (hydrophobic subunits) are maintained in the bilayer structure (supramolecular membranes).¹⁵ The hydrogen-bond networks present in the bilayer are stabilized by their stacking, similar to the case of nucleic acid base pairs in DNA. These findings prompted us to investigate their reconstitution in water. We herein provide an example that the complementary hydrogen-bond networks are in situ-formed in water and undergo hierarchical self-assembly into supramolecular membranes. The amphiphilicities, chemical structures of the complementary pairs, and the aqueous environment exert decisive roles in the complexation process and in the structural characteristics of reconstituted assemblies.

Results and Discussion

Complementary Molecular Subunits for the Hybridization in Water. To promote the formation of complementary hydrogen bonds in water, we propose to use the complementary subunits that acquire amphiphilicity upon formation of the hydrogen bonds. It is expected that such in situ-formed

(9) (a) Constant, J. F.; Fahy, J.; Lhomme, J. Anderson, J. E. *Tetrahedron Lett.* **1987**, 28, 1777. (b) Rotello, V. M.; Viani, E. A.; Deslongchamps, G.; Murray, B. A.; Rebek, J., Jr. *J. Am. Chem. Soc.* **1993**, 115, 797. (c) Kato, Y.; Conn, M.; Rebek, J., Jr. *Proc. Natl. Acad. Sci. U.S.A.* **1995**, 92, 1208.

(10) (a) Nowick, J. S.; Chen, J. S. *J. Am. Chem. Soc.* **1992**, 114, 1107. (b) Nowick, J. S.; Chen, J. S.; Noronha, G. *J. Am. Chem. Soc.* **1993**, 115, 7636. (c) Nowick, J. S.; Cao, T.; Noronha, G. *J. Am. Chem. Soc.* **1994**, 116, 3285.

(11) Hirschberg, J. H. K. K.; Brunsfeld, L.; Ramzi, A.; Vekemans, J. A. J. M.; Sijbesma, R. P.; Meijer, E. W. *Nature* **2000**, 407, 167.

(12) (a) Kurihara, K.; Ohto, K.; Honda, Y.; Kunitake, T. *J. Am. Chem. Soc.* **1991**, 113, 5077. (b) Ikeura, Y.; Kurihara, K.; Kunitake, T. *J. Am. Chem. Soc.* **1991**, 113, 7343. (c) Sasaki, D. Y.; Kurihara, K.; Kunitake, T. *J. Am. Chem. Soc.* **1992**, 114, 10994. (d) Taguchi, K.; Ariga, K.; Kunitake, T. *Chem. Lett.* **1995**, 701. (e) Cha, X.; Ariga, K.; Kunitake, T. *J. Am. Chem. Soc.* **1996**, 118, 9545. (f) Koyano, H.; Bissel, P.; Yoshihara, K.; Ariga, K.; Kunitake, T. *Chem. Eur. J.* **1997**, 3, 1077 and references therein.

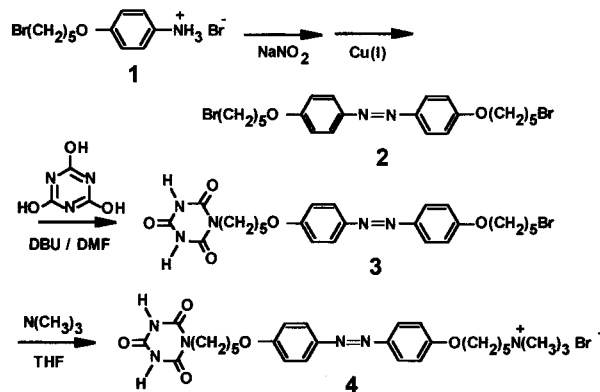
(13) (a) Kitano, H.; Ringsdorf, H. *Bull. Chem. Soc. Jpn.* **1985**, 58, 2826. (b) Ahlers, M.; Ringsdorf, H.; Rosemeyer, H.; Seela, F. *Colloid Polym. Sci.* **1990**, 268, 132. (c) Ahuja, R.; Caruso, P.-L.; Möbius, D.; Paulus, W.; Ringsdorf, H.; Wildburg, G. *Angew. Chem., Int. Ed. Engl.* **1993**, 32, 1033. (d) Bohanon, T. M.; Denzinger, S.; Fink, R.; Paulus, W.; Ringsdorf, H.; Weck, M. *Angew. Chem., Int. Ed. Engl.* **1995**, 34, 58. (e) Ebara, Y.; Itakura, K.; Okahata, Y. *Langmuir* **1996**, 12, 5166.

(14) Onda, M.; Yoshihara, K.; Koyano, H.; Ariga, K.; Kunitake, T. *J. Am. Chem. Soc.* **1996**, 118, 8524.

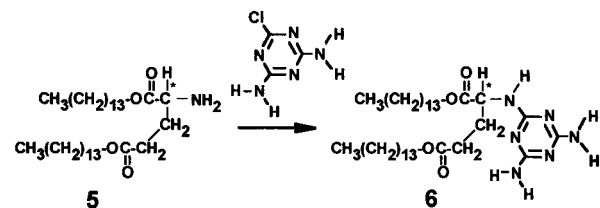
(15) (a) Kimizuka, N.; Kawasaki, T.; Kunitake, T. *J. Am. Chem. Soc.* **1993**, 115, 4387. (b) Kimizuka, N.; Kawasaki, T.; Kunitake, T. *Chem. Lett.* **1994**, 33. (c) Kimizuka, N.; Kawasaki, T.; Kunitake, T. *Chem. Lett.* **1994**, 1399. (d) Kimizuka, N.; Kawasaki, T.; Hirata, K.; Kunitake, T. *J. Am. Chem. Soc.* **1998**, 120, 4094.

(16) (a) Kimizuka, N.; Kawasaki, T.; Hirata, K.; Kunitake, T. *J. Am. Chem. Soc.* **1995**, 117, 6360. (b) Kimizuka, N.; Fujikawa, S.; Kuwahara, H.; Kunitake, T.; March, A.; Lehn, J.-M. *J. Chem. Soc., Chem. Commun.* **1995**, 2103.

Scheme 1



Scheme 2



“amphiphilic” hydrogen-bond pairs further self-assemble into the higher supramolecular architectures. As the complementary hydrogen-bond subunits, we have chosen the amphiphilic pair of melamine and cyanuric acid.¹⁵ Azobenzene chromophore was introduced in the cyanurate subunit (**4**, Scheme 1), to spectrophotometrically monitor the hybridization process. We have reported that the incorporation of an aromatic segment dramatically enhances the stability of the *preformed* hydrogen-bond networks in water.¹⁵ Azobenzene chromophores in the bilayer assemblies display unique spectral characteristics depending on their orientation,¹⁷ and the *trans*-to-*cis* photoisomerization of the chromophore provides a unique opportunity to investigate the role of molecular stereochemistry in the complexation process. As the hydrophobic subunit, L- or D-glutamate-derivatized melamine **2C₁₄-L-(or D)-Glu-Mela** (**6**) was employed (Scheme 2). It is reported that self-assembly of chiral amphiphiles often leads to the formation of helical nanostructures,¹⁸ and such a morphology is only available through the hierarchical self-assembly of the complementary subunits.

Electron Microscopy. Transmission electron micrographs of the single component **4** (a), **6**(D-form) (b) and the mixtures of **6**(D-)–**4** (1:1) (c), **6**(D-)–**4** (3:1) (d) in water are shown in Figure 1. The melamine derivative **6** was added from ethanol stock solutions, and the ethanol content in the presence of **6** was adjusted to 10 vol %. Aqueous dispersion of **4** alone displayed globular aggregate structures with diameters of 30–50 nm (Figure 1a). On the other hand, when the ethanolic solution of **6**(D-) was injected in water, irregular ellipsoidal aggregates with long axes of 40–130 nm were observed (Figure 1b). As the solution was homogeneous at this concentration, it seems that the melamine and glutamate moiety served as a hydrophilic group to ensure the solubility.

Surprisingly, when **6**(D-) and **4** were mixed in water at an equimolar ratio, helical superstructures with thicknesses of 14–

(17) (a) Shimomura, M.; Ando, R.; Kunitake, T. *Ber. Bunsen-Ges. Phys. Chem.* **1983**, 87, 1134. (b) Shimomura, M.; S. Aiba; Tajima, N.; Inoue, N.; Okuyama, K. *Langmuir* **1995**, 11, 969. (c) Song, X.; Perlstein, J.; Whitten, D. G. *J. Am. Chem. Soc.* **1997**, 119, 9144.

(18) (a) Nakashima, N.; Asakuma, S.; Kunitake, T. *J. Am. Chem. Soc.* **1985**, 107, 509. (b) Nakashima, N.; Asakuma, S.; Kim, J.-M.; Kunitake, T. *Chem. Lett.* **1984**, 1709.

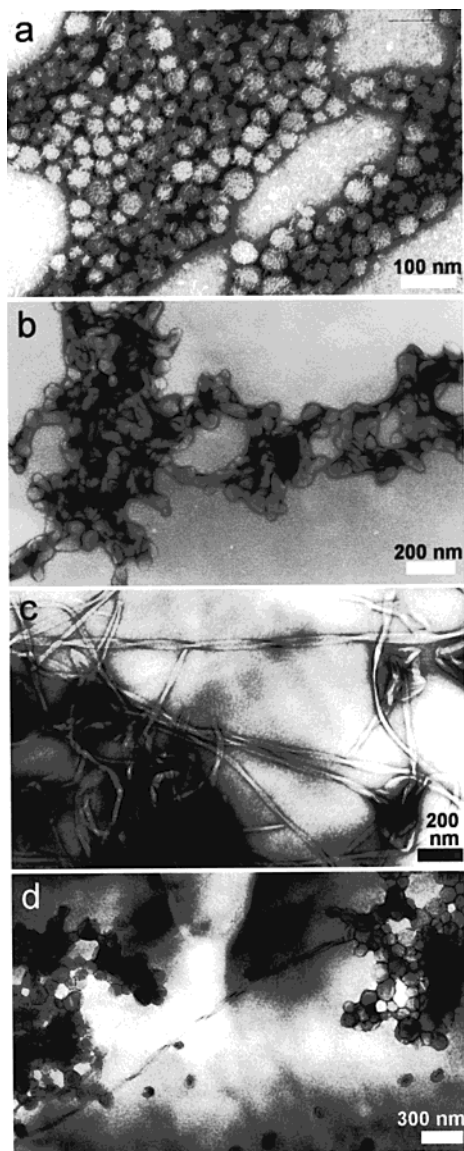


Figure 1. Electron micrographs of aqueous dispersions. (a) **4**, (b) **6(D-)**, (c) **6(D-):4 = 1:1**, (d) **6(D-):4 = 3:1**. Content of ethanol, (a) 0 vol %, (b)–(d) 10 vol %. Samples were stained by uranyl acetate.

28 nm, widths of 30–50 nm, and pitches of 180–430 nm were observed (Figure 1c). These helical structures are stably dispersed in water and are apparently distinct from those observed for the individual subunits (Figure 1a, b). In addition, they are observed in the wide ethanol concentrations (from 2.5 to 50 vol %). We have reported that such helical superstructures are typically formed from the highly ordered, chiral bilayer membranes.¹⁸ Therefore, nanohelices in Figure 1c most likely are comprised of supramolecular membranes that are hierarchically self-assembled from the in situ-formed, amphiphilic complementary hydrogen-bond networks **6–4**. A similar helical superstructure was obtained when **6(L-form)** was employed in place of the D-form. Interestingly, when both components were mixed at a molar ratio of **6(D-):4 = 3:1**, globular structures characteristic of the self-aggregates of **6(D-)** were observed, in addition to the helical structures (Figure 1d). These observations suggest that the complexation of complementary subunits is stoichiometric and excess subunit molecules are not incorporated in the reconstituted assembly.

UV–Vis Spectra and Induction of Circular Dichroism.

Figure 2 displays UV–vis absorption spectra (a) and CD spectra

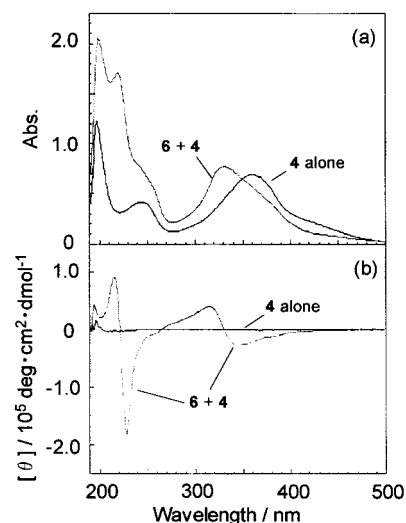


Figure 2. UV–vis spectra (a) and CD spectra (b) of aqueous **4** in the absence and presence of **6(L-)**. [**6(L-)**] = [**4**] = 5×10^{-5} M, ethanol; 20 vol %, 20 °C.

(b) of **4** in the absence and presence of equimolar **6(L-)** in water (concentration of ethanol, 20 vol %). The hydrogen-bond-mediated supramolecular membrane is stable toward lysis up to the concentration of 50 vol % ethanol, as will be discussed later. The absorption peaks of azobenzene chromophore near 240 and 360 nm are associated with the $\pi-\pi^*$ transition moment along the short and long axes, respectively.^{17a} The long-axis absorption band of **4** alone in water is observed at 360 nm (Figure 2a), and this λ_{\max} is identical with that observed for the molecularly dispersed azobenzene chromophores in alcoholic solution, in micellar aggregates, or in liquid crystalline bilayers.^{17a} Upon heating the aqueous dispersion from 30 to 80 °C, the absorption displayed a gradual intensity increase up to 35% of the initial intensity (data not shown). The observed hypochromism at lower temperature is indicative of a weak electronic interaction among azobenzene chromophores, which is characteristically observed for micellar aggregates.^{17a}

Interestingly, upon the addition of equimolar **6(L-)**, the absorption peak of **4** at 360 nm showed an immediate blue-shift to 330 nm (Figure 2a). Such a blue-shifted absorption has been observed for ordered azobenzene bilayers¹⁷ and is ascribed to the strong exciton interaction among the regularly aligned transition dipoles in the assembly.¹⁹ This is consistent with the observation of developed helical superstructures in Figure 1c. Furthermore, a sharp peak is observed at 219 nm, in addition to the shoulder component of azobenzene short-axis transition at 240 nm. The 219-nm band is red-shifted compared to the absorption λ_{\max} of **6(D-)** alone in ethanol (208 nm), and this also originates from the exciton interaction among the melamine units aligned in the linear complementary hydrogen-bond networks.^{19,20a}

Circular dichroism of these aqueous solutions was investigated to demonstrate the presence of excitonic interactions (Figure 2b). Naturally, no CD peak was observed for the achiral subunit **4** alone in water. On the other hand, upon the addition of subunit **6(L-)** to the aqueous solution of **4**, two intense couples

(19) (a) Kasha, M. In *Spectroscopy of the Excited State*; Bartolo, B. D., Ed.; Plenum Press: New York, 1976; p 337. (b) Kasha, M. Rawls, H. R.; El-Bayoumi, M.; *Pure Appl. Chem.* **1965**, *11*, 371.

(20) (a) Tokuhiko, M. Masters Thesis, Kyushu University, 1998. (b) ICD component for the azobenzene-short axis band (λ_{\max} at 240 nm) is not included in these peaks since it is located in the longer wavelength and the magnitude of exciton interaction among azobenzene short-axis transition dipoles are weak, as reported for chiral azobenzene bilayers.^{22c}

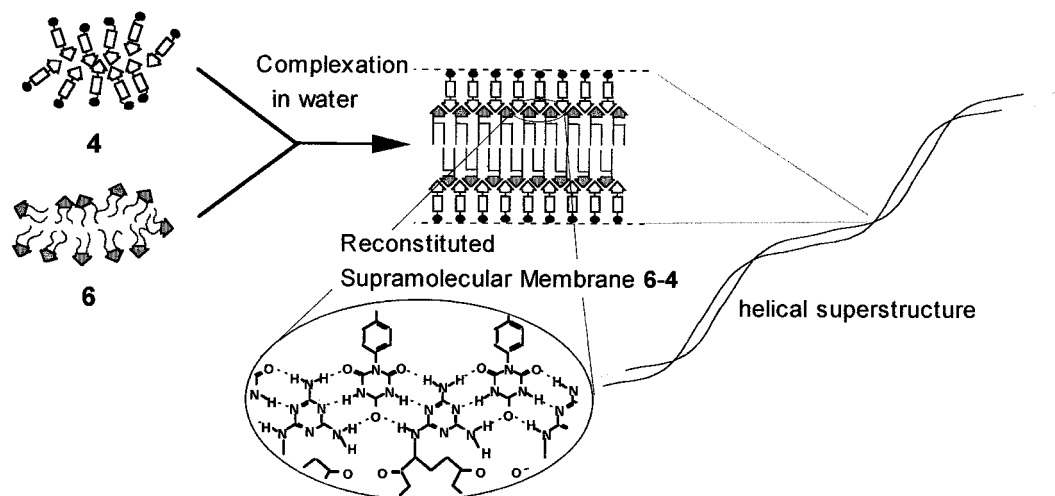


Figure 3. Schematic illustration of the hybridization of amphiphilic complementary hydrogen-bond networks **6-4** in water and their hierarchical self-assembly into supramolecular membranes. Chirality in the melamine subunit **6** is expressed as helical superstructures of the reconstituted assembly.

of positive and negative Cotton effects appeared. A mirror-symmetric CD spectrum was obtained when **6** (D-) was employed in place of the L-form. The positive and negative peaks at 216 nm ($[\theta] = +9.1 \times 10^4 \text{ deg}\cdot\text{cm}^2\cdot\text{dmol}^{-1}$) and 228 nm ($[\theta] = -1.8 \times 10^5 \text{ deg}\cdot\text{cm}^2\cdot\text{dmol}^{-1}$), and those at 315 nm ($[\theta] = +4.0 \times 10^4 \text{ deg}\cdot\text{cm}^2\cdot\text{dmol}^{-1}$) and 346 nm ($[\theta] = -2.8 \times 10^4 \text{ deg}\cdot\text{cm}^2\cdot\text{dmol}^{-1}$) are characteristic of the exciton coupling,²¹ and they indicate the presence of strong excitonic interaction among the $\pi-\pi^*$ transition dipoles of melamine and azobenzene chromophores, respectively. According to a semi-quantitative application of Kasha's molecular exciton theory,¹⁹ the blue-shift of azobenzene absorption observed upon mixing the subunits (Figure 2a) is ascribed to the parallel orientation of the chromophores in the assembly.

It is noteworthy that the exciton coupling is induced in the absorption band of achiral azobenzene subunit. Apparently, structural information of the chiral melamine subunit is effectively transferred to the azobenzene subunit. Generally, a magnitude of induced circular dichroism (ICD) is inversely proportional to the third power of the distance between a chiral molecule and an achiral chromophore.²³ The appearance of such an intense exciton-coupled ICD, then, must be ascribed to the regularly fixed orientation of azobenzene group against the glutamate moiety and to the resultant extensive delocalization of photoexcitation energy over the oriented azobenzene chromophores. Such regular supramolecular organization of two subunits should be possible only via the formation of complementary hydrogen bonds. The positive and negative Cotton effects at 216 and 228 nm are ascribed to the exciton interaction among the melamine subunits,²⁰ and are clearly distinguishable from the CD spectrum observed for the self-aggregates of **6**(D-)(data not shown, $[\theta]_{201} = +6.5 \times 10^4 \text{ deg}\cdot\text{cm}^2\cdot\text{dmol}^{-1}$, $[\theta]_{216} = -1.2 \times 10^5 \text{ deg}\cdot\text{cm}^2\cdot\text{dmol}^{-1}$, 18 h after injection of the ethanol solution in water). These spectral observations, together with the formation of helical superstructures, clearly indicate that the highly ordered supramolecular membranes are reconstituted by complementary hydrogen bonding in water.

In contrast to the observed immediate blue-shift in the azobenzene absorption upon mixing the complementary subunits, the intensity of the corresponding ICD peaks observed just after mixing was about 65% of the maximum value (Figure 2b), the intensity of which was attained after ca. 1.5 h. The

observed slow increase in the ICD intensity is indicative of the molecular ordering process in the reconstituted supramolecular membrane.

It is interesting to compare these spectral characteristics with those observed for the *preformed* supramolecular membranes.¹⁵ In the previous studies, the complementary pairs were prepared by mixing equimolar subunits in organic solvents. The complementary hydrogen-bond pairs obtained after the removal of solvents were successively dispersed in water by ultrasonication.¹⁵ Aqueous dispersion of the preformed supramolecular membrane **6**(L)-**4** thus prepared possessed an absorption λ_{max} at 339 nm and ICD intensities of $[\theta]_{330} = +1.6 \times 10^4 \text{ deg}\cdot\text{cm}^2\cdot\text{dmol}^{-1}$ and $[\theta]_{365} = -4.8 \times 10^3 \text{ deg}\cdot\text{cm}^2\cdot\text{dmol}^{-1}$, respectively (20 °C). The observed absorption blue-shift and the ICD intensities are less eminent compared to those of the in situ-formed assembly (Figure 2). The larger ICD intensities observed for the reconstituted assembly must reflect the improved molecular orientation. The less ordered molecular alignment in the preformed membrane **6**(L)-**4** is also reflected in the lower population of helical structures observed by electron microscopy.^{15c} Ultrasonication of aqueous bilayers is known to produce defects,²⁴ and the in situ complexation technique, which is devoid of such a deteriorating effect, thus provides supramolecular membranes with the improved molecular order.

The present reconstitution process is schematically shown in Figure 3. By mixing the suitably designed complementary subunits **4**, **6** in water, amphiphilic networks of the linear complementary hydrogen bonds **6-4** are spontaneously formed, and they simultaneously self-integrate into the supramolecular membranes. Water plays an essential role to direct the hydrogen bonding and their hierarchical molecular organization. At first, the self-aggregates of **6** collide and fuse with the globular self-aggregates of **4**, presumably due to hydrophobic interactions.

(21) Harada, N.; Nakanishi, K. *Circular Dichroic Spectroscopy: Exciton Coupling in Organic Stereochemistry*; University Science Books: Mill Valley, CA, 1983.

(22) (a) Kunitake, T.; Nakashima, N.; Shimomura, M.; Okahata, Y.; Kano, K.; Ogawa, T. *J. Am. Chem. Soc.* **1980**, *102*, 6644. (b) Kunitake, T.; Nakashima, N.; Morimitsu, K. *Chem. Lett.* **1980**, 1347. (c) Nakashima, N.; Morimitsu, K.; Kunitake, T. *Bull. Chem. Soc. Jpn.* **1984**, *57*, 3253.

(23) Craig, D. P.; Power, E. A.; Thirunamachandran, T. *Chem. Phys. Lett.* **1974**, *27*, 149.

(24) Szoka, F., Jr.; Papahadjopoulos, D. *Annu. Rev. Biophys. Bioeng.* **1980**, *9*, 467.

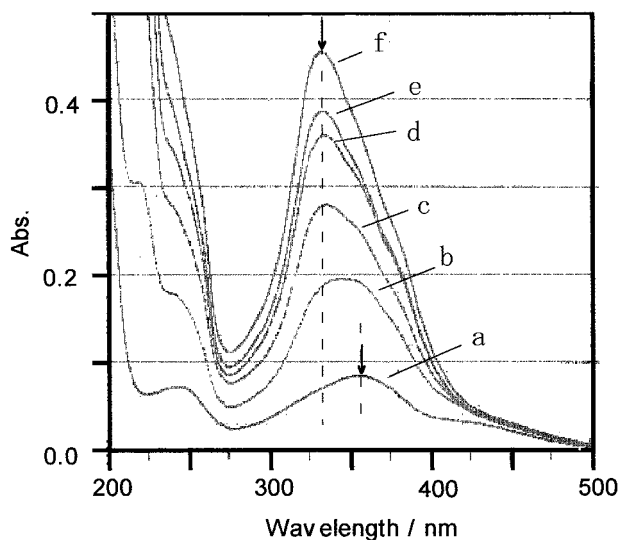


Figure 4. UV-vis spectra of aqueous **4** at varied molar ratio of **6(D-)**. **4**: **6(L-)** = (a) 1:0, (b) 1:0.2, (c) 1:0.4, (d) 1:0.6, (e) 1:0.8, (f) 1:1. **[4]** = 2.5×10^{-5} M, ethanol; 5 vol %, 20 °C.

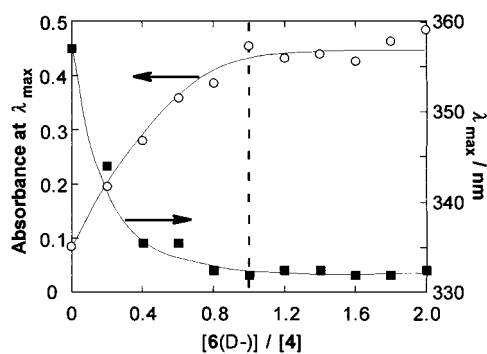


Figure 5. Dependence of absorption maximum (■) and its intensity (○) on the molar ratio of complementary subunits. **[4]** = 2.5×10^{-5} M, ethanol; 5 vol %, 20 °C.

Subsequently, complementary hydrogen-bond networks are formed in the mixed aggregates. The presence of bulk water directs the supramolecular organization, in which the more hydrophobic melamine subunits are organized in the interior of the assembly and the ammonium-containing counterparts constitute the outer surface of the assembly. This amphiphilic supramolecular organization satisfies both the solubility and the maintenance of the complementary hydrogen-bond networks in water. These hydrogen bonds are effectively shielded from the bulk water by their packing in the bilayer. The observed hydrophobically driven supramolecular organization is reminiscent of the biological self-assemblies and the protein folding.

Determination of the Stoichiometry and Association Constant. To confirm the stoichiometry and to determine the association constant of the complexation process, spectral titration experiments were conducted for the pair of **6(D-)** and **4**. Figure 4 displays absorption spectra of **4** (2.5×10^{-6} M) in the presence of **6(D-)** at varied molar ratios. With increasing the molar ratio of **6(D-)**, absorption λ_{\max} initially located at 357 nm for **4** alone shifted to 332 nm, and this spectral blue-shift was accompanied by an increase in the absorption intensity. In Figure 5, absorption λ_{\max} of **4** and its peak intensity are plotted against the molar ratio $[\mathbf{6(D-)}]/[\mathbf{4}]$. Both the spectral blue-shift and absorbance increase leveled off near the equimolar ratio, indicating that the reconstitution occurs stoichiometrically. This

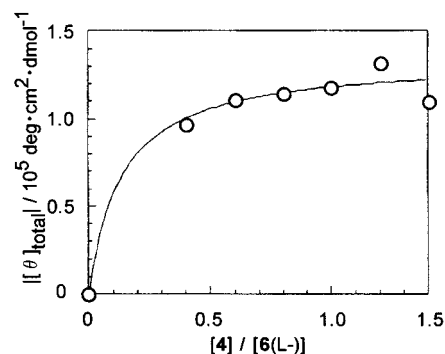


Figure 6. Dependence of $[\theta]_{\text{total}}$ on the molar ratio of complementary subunits. $[\mathbf{6(L-)}] = 5 \times 10^{-5}$ M, ethanol; 20 vol %, 20 °C.

is consistent with the observed segregation of excess subunits from the reconstituted helical superstructures (Figure 1d).

In Figure 6, ICD intensity ($[\theta]_{\text{total}} = |[\theta]_{315}| + |[\theta]_{346}|$) obtained for **6(L-)-4** is plotted against the molar ratio of $[\mathbf{4}]/[\mathbf{6(L-)}]$. The ICD intensity also reached a constant value near the composition of $\mathbf{4}/\mathbf{6(L-)} = 1/1$. The magnitude of association constant K was determined according to the Benesi–Hildebrand equation and by the least-squares fitting.

$$1/\Delta[\theta]_{\text{obsd}} = ([1/K]\Delta[\theta]_{\text{total}})/C_{\text{azo}} + 1/\Delta[\theta]_{\text{total}} \quad (1)$$

where

$$C_{\text{azo}} = [\mathbf{4}] \text{ in mol}\cdot\text{L}^{-1} \quad (2)$$

Analysis of the data in Figure 6 indicates that **4** binds to **6(L-)** with an association constant of $1.13 \times 10^5 \text{ M}^{-1}$. This value is significantly larger than those reported for the hydrogen bonding in aqueous media (binding of hexylthymine to acetylpenhthyladenine in SDS micelle; $K = 48 \text{ M}^{-1}$)^{10c} or at the air–water interface (barbituric acid to a surface monolayer of dialkylated melamine^{12f}; 2530 M^{-1} , 2,4,6-triaminopyrimidine to a cyanurate lipid monolayer^{13e}; 3500 M^{-1}). It is clear that formation of the complementary hydrogen-bond-mediated bilayer in aqueous media is much facilitated, compared to the previously reported aqueous and surface monolayer systems.

Effect of Ethanol Content on the Molecular Organization.

Generally, water-miscible organic solvents such as ethanol cause lyses of aqueous bilayer membranes.^{24,25} Since melamine subunits are injected into water from ethanol solutions, the effect of ethanol concentration on the reconstituted bilayer was investigated. Figure 7 displays UV-vis absorption (a) and CD spectra (b) of **6(L-)-4** that has been reconstituted at varied ethanol concentrations. Below the ethanol content of 20 vol %, absorption λ_{\max} of azobenzene chromophore is located at 330 nm (parallel chromophore orientation), while the absorption at 360 nm starts to increase above the ethanol content of 40 vol %. When 50 vol % of ethanol is present, spectral intensities at 330 and 360 nm become almost identical. By further increasing the ethanol content to 70 vol %, complete shift of the absorption peak to 357 nm was observed. In addition, a sharp absorption peak at 220 nm, which is ascribed to the melamines organized in the hydrogen-bond network, showed a decrease upon increasing the ethanol content and completely disappeared at 70 vol %. The absorption peaks observed at 70 vol % ethanol (357 nm for azobenzene, 206 nm for melamine) are almost identical

(25) (a) Dalton, A. D.; Miller, K. W. *Biophys. J.* **1993**, *65*, 1620. (b) Regen, S. L.; Czech, B.; Singh, A. *J. Am. Chem. Soc.* **1980**, *102*, 6638. (c) Roks, M. F. M.; Visser, H. G. J.; Zwicker, J. W.; Verkley, A. J.; Nolte, R. *J. J. Am. Chem. Soc.* **1983**, *105*, 4507.

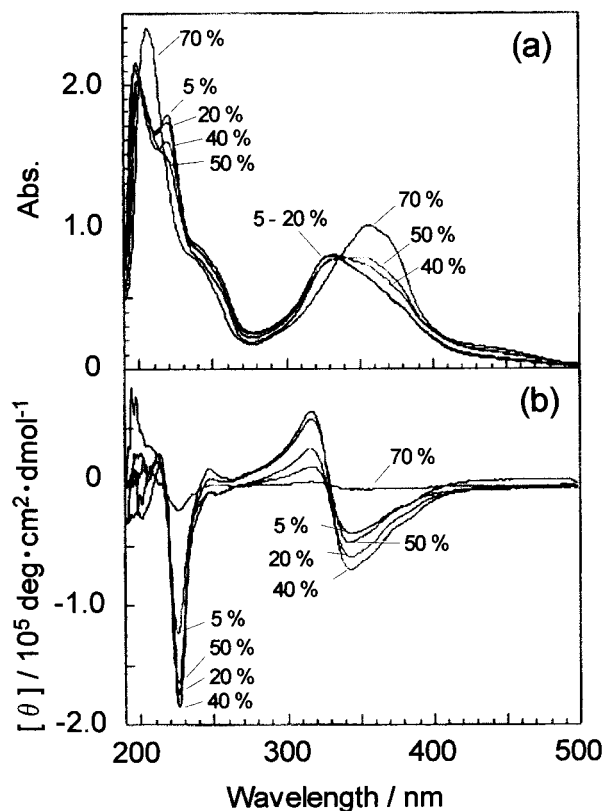


Figure 7. UV-vis (a) and CD (b) spectra of aqueous **6(L-)-4** at varied ethanol concentrations. $[4] = [6(L-)] = 5 \times 10^{-5}$ M, 20 °C.

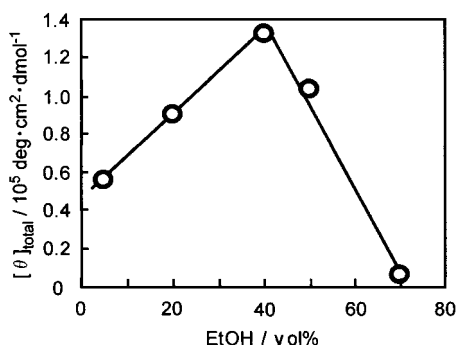


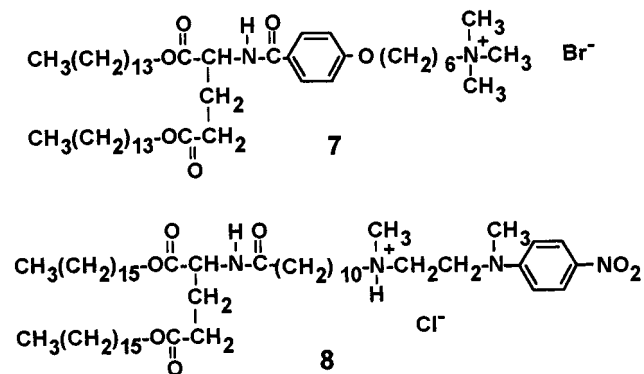
Figure 8. Dependence of ICD intensity $[\theta]_{\text{total}}$ on the ethanol concentration.

to those of the isolated chromophores, and these observations indicate that the supramolecular membrane is lysed at this ethanol concentration.

Interestingly, the magnitude of ICD spectra $[\theta]_{\text{total}}$ ($= |[\theta]_{315}| + |[\theta]_{346}|$) in **6(L-)-4** (Figure 7b) showed a unique dependence on the ethanol concentration. It increased with ethanol concentration and reached a maximum at ca. 40 vol % (Figure 8). Further increase in ethanol content results in a decrease in the $[\theta]_{\text{total}}$ value, and it almost disappeared at 70 vol %. Similarly, CD intensity at 225 nm reached a maximum value at the ethanol concentration of 40 vol % and is considerably weakened at 70 vol %. Consistent with these spectral observations, the developed helical superstructure was not observed by electron microscopy when the ethanol content exceeded 60 vol %.

As described previously, the intensity of the exciton-coupled CD reflects regularity of chiral molecular assembly, and therefore the reconstituted bilayer **6(L-)-4** possesses the highest molecular orientational order at the ethanol content of 40 vol %. This tendency is in remarkable contrast with the conventional

Chart 1



bilayer membranes such as **7**, which are lysed in the presence of 20–30 vol % ethanol^{26a} (see Chart 1).

We have reported that stable bilayer membranes were formed in binary aqueous–organic media when the amphiphile contains aromatic chromophores such as *N*-methyl-*p*-nitroaniline in the headgroup.²⁶ The amphiphile **8** adopts highly ordered “tilt” orientation in the presence of 40–60 vol % ethanol, and its molecular orientational order, as estimated from the intensity of CD spectra, is superior to that observed in pure water. Stabilization of diacylene-containing bilayers by ethanol has been also reported by other researchers.²⁷ The improved molecular alignment in the presence of ethanol may be a feature common to the bilayers with enhanced hydrophobicity and crystallinity.²⁶ Strong stacking of complementary hydrogen-bond networks and of azobenzene chromophores in **6-4** might be relaxed with the moderate ethanol concentration, which lowered the dielectric constant of the solvent and allowed their ordering in the assemblies.

Effect of trans-to-cis Photoisomerization of Azobenzene Unit on the Hybridization. The trans-to-cis photoisomerization of azobenzene chromophores in bilayers is influenced by the physical state of the membranes, and it is suppressed when bilayers are in rigid, gel state.²⁸ Figure 9 shows spectral absorption changes of the aqueous single component **4** upon UV-irradiation and the succeeding time dependence in the dark. Before photoirradiation (Figure 9a), the absorption peak is observed at 360 nm as described previously. Upon irradiation, the peak intensity at 360 nm decreases and new peaks appear at 430 and 326 nm, which are ascribable to the $n-\pi^*$ and $\pi-\pi^*$ transitions of the *cis*-isomer, respectively (Figure 9b). This spectral change was complete within 10 min. The photoirradiated spectrum (Figure 9b) possesses an absorption component around at 360 nm, which is attributable to the **4(trans)** species that remains in the dispersion. The fraction of *cis*-isomer in the photostationary state is ca. 85 mol %, as estimated by the absorption decrease at 360 nm. When the photoirradiated dispersion of **4** was kept in the dark, a slow increase in absorbance at 360 nm was observed, and 74% of the original intensity was attained in 25 h at 20 °C. Thus, the subunit **4** in the aqueous dispersion undergoes both the trans-to-cis photoisomerization and cis-to-trans thermal isomerization. The observed facile

(26) (a) Kimizuka, N.; Wakiyama, T.; Miyauchi, H.; Yoshimi, T.; Tokuhira, M.; Kunitake, T. *J. Am. Chem. Soc.* **1996**, *118*, 5808. (b) Kimizuka, N.; Tokuhira, M.; Miyauchi, H.; Wakiyama, T.; Kunitake, T. *Chem. Lett.* **1997**, 1049.

(27) (a) Schunur, J. M.; Ratna, B. R.; Selinger, J. V.; Singh, A.; Jyothi, G.; Easwaran, K. R. K. *Science* **1994**, *264*, 945. (b) Yamamoto, T.; Satoh, N.; Onda, T.; Tsujii, K. *Langmuir* **1996**, *12*, 3143.

(28) (a) Shimomura, M.; Kunitake, T. *J. Am. Chem. Soc.* **1987**, *109*, 5175. (b) Kunitake, T.; Okahata, Y.; Nakashima, N.; Shimomura, M.; Kano, K.; Ogawa, T. *J. Am. Chem. Soc.* **1980**, *102*, 6642.

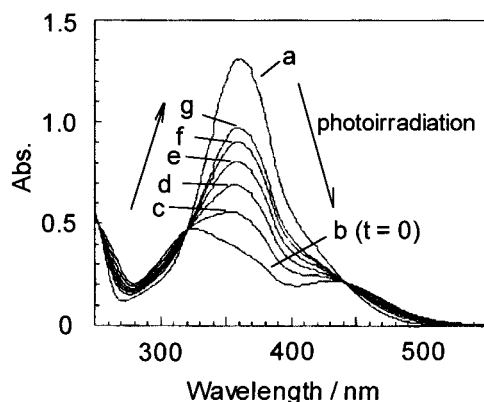


Figure 9. Effect of photoirradiation on the UV–Vis spectra of aqueous subunit **4** and succeeding spectral changes. (a) before photoirradiation, (b) just after photoirradiation, $t = 0$, (c) $t = 5$ h, (d) $t = 10$ h, (e) $t = 15$ h, (f) $t = 20$ h, (g) $t = 25$ h. $[4] = 5.2 \times 10^{-5}$ M, ethanol; 16 vol %, 20 °C.

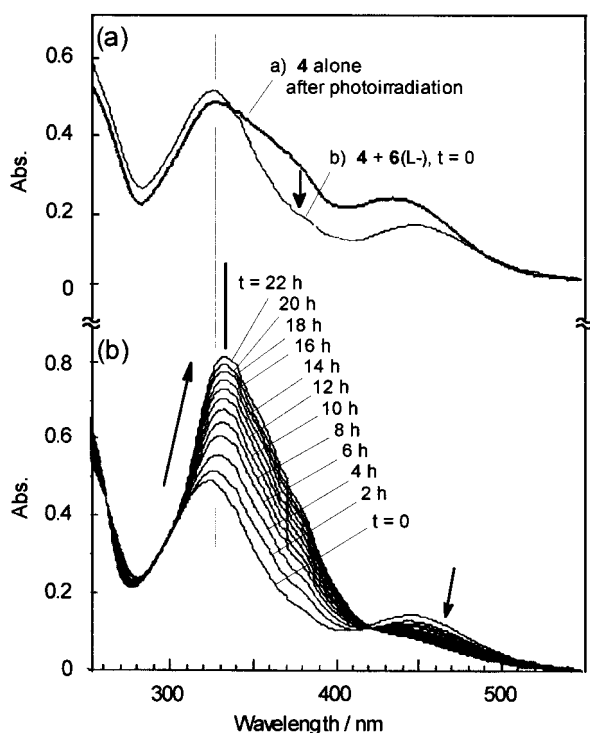


Figure 10. Effect of the addition of **6(L-)** to the UV–vis spectra of aqueous **4**. (a) a) after photoirradiation (the same spectrum as Figure 9b). b) equimolar **6(L-)** was added to the solution ($t = 0$). (b) time dependence after the addition of **6(L-)**. **6(L-)** was added at $t = 0$. $[4] = [6(L-)] = 5 \times 10^{-5}$ M, ethanol; 20 vol %, 20 °C.

photoisomerization of **4** is consistent with the formation of fluid, micellar self-aggregates.

Figure 10a shows absorption spectral change of photoirradiated **4** after the addition of equimolar subunit **6(L-)**. A rapid decrease in the spectral component at 350–450 nm was observed ($t = 0$), which is accompanied by a slight absorption increase at 324 nm. The rapid spectral decrease is ascribed to the hybridization between the coexisting **4(trans)**, λ_{\max} at 360 nm) and **6(L-)**, as inferred from their efficient complexation in water (Figure 2). This is also supported by the increase at 324 nm, which is close to the λ_{\max} of aqueous **6(L-)-4**. In Figure 10b, time dependence of the absorption spectra was recorded. The intensity of the $n-\pi^*$ absorption band (*cis*-isomer, at 444 nm) showed gradual decrease, indicating the progress of *cis*-

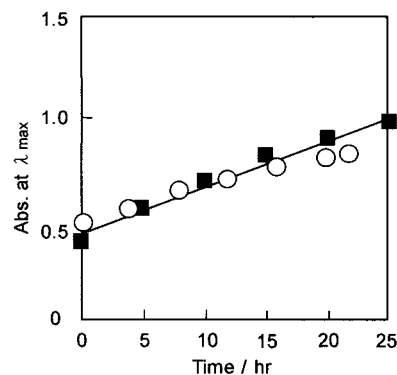


Figure 11. Time dependence of absorption increase after photoirradiation. (■): aqueous single component **4**, absorbance at 360 nm. (○): aqueous dispersion of **6(L-)-4**, absorbance at 330 nm. 20 °C.

to-*trans* thermal isomerization. The $\pi-\pi^*$ transition peak observed at 324 nm ($t = 0$) showed an increase in the intensity, and this was accompanied by a small spectral red-shift to 332 nm. This absorption λ_{\max} is distinct from that of the single component **4** (*trans*, λ_{\max} 360 nm), and is characteristic to the reconstituted bilayer **6(L-)-4(trans)**.

In Figure 11, the time course of the absorption increase at 330 nm is plotted together with those observed for the photoirradiated single component **4** (λ_{\max} at 360 nm, Figure 9). In the latter case, the *cis*-to-*trans* isomerization of aqueous **4** proceeds almost linearly with time (○). Interestingly, the absorbance increase at 330 nm (■) almost coincides with the time dependence of the *cis*-to-*trans* isomerization of **4** alone. Therefore, the *cis*-to-*trans* thermal transition of the component **4** is the rate-determining step in the reconstitution process, and the reconstitution proceeds selectively with the *trans*-form. It is interesting that the *cis*-form is not recognized as a complementary subunit. Apparently, the ability to form regular molecular alignment is required in the reconstitution process.

On the other hand, when photoillumination was conducted for the reconstituted bilayer of **6(L-)-4**, absorption intensity decrease (λ_{\max} at 332 nm) observed after photoirradiation (5 min) was only ca. 18% of the initial intensity (data not shown). This is accompanied by a slight absorption increase at 440 nm ($n-\pi^*$ band of the *cis*-form), and the spectrum was unchanged even after the prolonged irradiation of 20 min. Clearly, *trans*-to-*cis* photoisomerization of azobenzene chromophore is remarkably suppressed, once the subunit **4** is integrated in the supramolecular membrane **6(L-)-4**. By keeping the irradiated dispersion in the dark for 24 h, 96% of the initial absorption intensity at 332 nm recovered. This confirms that the *cis*-isomer formed in the bilayer is reversibly complexed with **6(L-)**, after the thermal *cis*-to-*trans* isomerization.

These observations are schematically illustrated in Figure 12. Upon the mixing of aqueous **4(trans)** and **6**, supramolecular membrane **6-4** is readily reconstituted in water (Figure 12a). Photoillumination of azobenzene unit in the single component **4(trans)** causes *trans*-to-*cis* isomerization (Figure 12b). The *cis*-isomer formed undergoes thermal isomerization back to the *trans*-form (Figure 12c). When the melamine subunit **6** is added to **4(cis)**, no-hybridization occurs with the *cis*-isomer (Figure 12d). On the other hand, the thermally regenerated subunit **4(trans)** undergoes immediate hybridization with **6**, and the supramolecular membrane **6-4** is formed (Figure 12g). The suppressed *trans*-to-*cis* photoisomerization observed for the reconstituted bilayer **6-4** clearly indicates that the supramolecular membrane is in the crystalline order (Figure 12h). Similar inhibition of *trans*-to-*cis* isomerization has been also observed

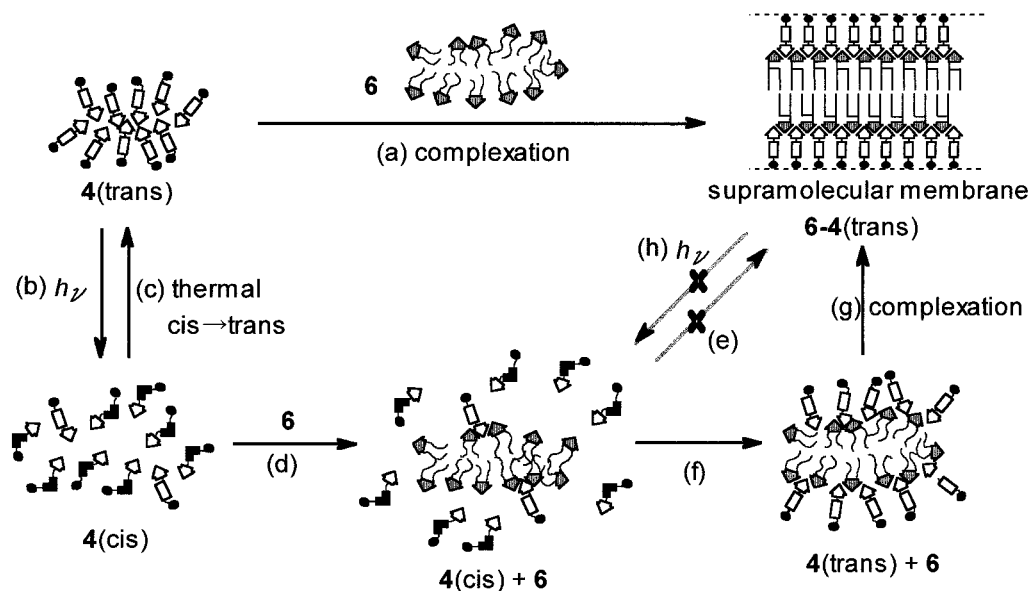


Figure 12. Schematic illustration of the complexation between subunits **6** and **4**. The effect of photoisomerization is also shown. (a) Supramolecular membrane is readily reconstituted in water from **4(trans)** and **6**. (b) Photoillumination of aqueous **4** causes trans-to-cis photoisomerization. (c) The photoisomerized **4(cis)** undergoes slow thermal isomerization to the trans form. (d, e) Addition of **6** to aqueous **4(cis)** leads to no hybridization. Only the *trans*-isomer coexisting in the solution is reconstituted into the supramolecular membrane **6-4**. (f) Thermal isomerization of **4(cis)** to **4(trans)** in the aqueous mixture. (g) Facile complexation between regenerated **4(trans)** and **6**. On the other hand, trans-to-cis photoisomerization of **4** is suppressed in the reconstituted bilayer **6-4** (h).

for the ordered assemblies of azobenzene-bilayers,²⁸ and also for the long-chain derivatives of thioindigo²⁹ and stilbene chromophores³⁰ in the monolayer films.

Conclusions

It is established that hydrogen-bond-mediated bilayer membranes are readily reconstituted in water by mixing the suitably designed complementary subunits. Both the single subunits form self-aggregates in water, and the hybridization process should involve collision and fusion of these aggregates as an initial step. Formation of complementary hydrogen-bond networks is remarkably facilitated in these mixed aggregates, and aqueous environment plays an indispensable role to direct the mode of hydrogen bonding into the linear, amphiphilic structure. They hierarchically self-assemble in water into the chiral supramolecular membranes, and stability of the hydrogen bonds is effectively secured by the integration. Participation of the aqueous environment to direct mesoscopic supramolecular assemblies has been a marked feature for the biological supramolecular assemblies. The present reconstitution of supramolecular membranes in aqueous media, together with the solvophobic directed mesoscopic supermolecules in organic media,¹⁶ provides a new generation of supramolecular chemistry.

Experimental Section

Materials. Glutamate derivatives of melamine and azobenzene-containing isocyanuric acid were synthesized according to Schemes 1 and 2. The structures of the intermediates and the final products were confirmed by thin-layer chromatography, IR and NMR spectroscopies, and elemental analysis. Isocyanuric acid (Tokyo Kasei), $\text{CuSO}_4 \cdot 5\text{H}_2\text{O}$ (Kishida Chemical), 2-chloro-4,6-diamino-1,3,5-triazine (Aldrich) were purchased and used as received. Ethanol used for spectral measurements was of spectral grade (Kishida Chemical).

2C₁₄-D-Glu-Mela (6). Tetradecyl D-glutamate (**5**) was synthesized according to the reported procedure.³¹ The ester (**5**) (67 mmol) was dissolved in chloroform and washed with aqueous Na_2CO_3 and with a

saturated solution of aqueous NaCl. The organic layer was separated and dried over Na_2SO_4 , and evaporation of the solvent afforded tetradecyl D-glutamate as an oily product. To this oil, 2-chloro-4,6-diamino-1,3,5-triazine (2.5 g, 17.2 mmol) was added, and the mixture was heated at 90 °C for 18 h. After cooling to room temperature, the crude product was extracted with chloroform and chromatographed on silica gel (30:1 → 20:1 CHCl_3 /methanol). Recrystallization from ethanol gave colorless powder (1.0 g, 9%). TLC (silica gel, CHCl_3) R_f = 0.03; IR (KBr) ν (N-H) 3470, 3380, ν (C-H) 2920, 2850, ν (C=O) 1730, ν (triazine) 815 cm^{-1} ; $^1\text{H NMR}$ (CDCl_3) δ 0.7–1.0 (t, 6H, CH_3), 1.0–1.6 (m, 48H, CH_2), 2.35 (m, 2H, NCH_2), 3.9–4.3 (m, 7H, NCHCO , CH_2COO , OCH_2), 4.81 (s, 4H, NH_2), 5.4–5.7 (d, 1H, NH). Anal. Calcd for $\text{C}_{36}\text{H}_{68}\text{O}_4\text{N}_6 \cdot 0.25 \text{H}_2\text{O}$: C, 66.17; H, 10.57; N, 12.86%. Found: C, 66.23; H, 10.53; N, 12.56%. The L-isomer was synthesized by refluxing 2-chloro-4,6-diamino-1,3,5-triazine and tetradecyl L-glutamate hydrochloride in the presence of KHCO_3 . Anal. Calcd for $\text{C}_{36}\text{H}_{68}\text{O}_4\text{N}_6$: C, 66.63; H, 10.56; N, 12.95%. Found: C, 66.63; H, 10.63; N, 12.89%.

4,4'-Bis[ω -bromopentyl]oxyazobenzene (2). *p*-[ω -Bromopentyl]oxyaniline hydrobromide (**1**) was prepared according to a previously reported procedure.^{17a} Ice-cooled aqueous NaNO_2 (1.7 g, 24.5 mmol) was cautiously poured into a stirred solution of *p*-[ω -bromopentyl]oxyaniline hydrobromide (8.4 g, 24.8 mmol) dissolved in 200 mL of water–acetone mixture (1/1 by volume) containing hydrochloric acid (35%, 2.7 g), and the mixture was kept below 5 °C. Separately, $\text{CuSO}_4 \cdot 5\text{H}_2\text{O}$ (6.3 g, 25.4 mmol) was dissolved in water (50 mL), and aqueous ammonia (28%) was added until the precipitate formed was dissolved. To the resultant dark blue solution, aqueous hydroxylamine hydrochloride (1.7 g, 24.9 mmol in 20 mL) was added to give a colorless mixture. As soon as the resultant colorless solution was poured into the diazonium salt solution, black precipitate was formed. Acetone was then added to the viscous reaction mixture, and stirring was continued for 1.5 h. After removal of acetone from the reaction mixture under reduced pressure, the crude product was extracted with chloroform. Purification was conducted by column chromatography on silica gel (eluent CHCl_3 , first elute was collected) to give 2.3 g (36%) of a reddish yellow powder: mp 122 → 141 °C (arrow indicates the liquid crystalline region); TLC (silica gel, CHCl_3) R_f 0.2; IR (KBr) ν (C-H) 2930, 2860 cm^{-1} , ν (N=N) 1680 cm^{-1} , ν (C-O-C) 1250 cm^{-1} .

(29) Whitten, D. G. *J. Am. Chem. Soc.* **1974**, *96*, 594.

(30) Whitten, D. G. *Acc. Chem. Res.* **1993**, *26*, 502.

(31) Asakuma, S.; Okada, H.; Kunitake, T. *J. Am. Chem. Soc.* **1991**, *113*, 1749.

N-{5-[*p*'-(5-Bromopenthyloxy)phenylazo]phenyloxy]pentyl}-cyanurate (**3**). (**2**) (2.3 g, 4.5 mmol) and isocyanuric acid (0.6 g, 4.6 mmol) were dissolved in 150 mL of DMF. 1,8-Diazabicyclo[5.4.0]undec-7-ene (DBU; 0.7 g, 4.6 mmol) was added to this solution, and the reaction mixture was heated at 60 °C for 14 h. After the reaction was terminated by the addition of water, the precipitate formed was filtered off, and the product was applied for column chromatography on silica gel (CHCl₃ → 29:1 CHCl₃/methanol) to give yellow powder of (0.25 g, 10%); mp 210–215 °C; TLC(CHCl₃/CH₃OH, 29:1) *R*_f 0.71; IR-(KBr) ν (N–H) 3200, 3050 cm⁻¹, ν (C–H) 2930, 2860 cm⁻¹, ν (C=O) 1770, 1680 cm⁻¹, ν (N=N) 1680 cm⁻¹, ν (C–O–C) 1250 cm⁻¹; ¹H NMR (3:1 CDCl₃/DMSO-*d*₆) δ 1.1–1.2 (m, 12H, CH₂), 3.42 (t, 2H, CH₂Br), 3.6–4.2 (t + t, 6H, OCH₂, N–CH₂), 6.7–8.0 (d + d, 8H, ph), 11.35 (s, 2H, NH).

N-{5-[*p*'-(5-Trimethylammonio-penthyloxy)phenylazo]-phenyloxy]pentyl}isocyanurate Bromide (**4**). (**3**) (0.25 g, 0.45 mmol) was dissolved in 50 mL of anhydrous THF. Gaseous trimethylamine (2.0 g, 33.9 mmol) was then dissolved in the solution, and the mixture was stirred for 9 days at room temperature. A precipitate formed with the progress of the reaction was collected and extracted with ethanol. After removing the solvent in vacuo, recrystallization from water afforded a yellow powder of **4** (0.05 g, 18%). ¹H NMR (DMSO-*d*₆/D₂O/CD₃OD) δ 1.3–2.1 (m, 12H, CH₂), 3.25 (m, 11H, N–CH₃, N–CH₂), 7.0–8.0 (d + d, 8H, ph). Anal. Calcd for C₂₈H₃₉O₅N₆Br·1.5H₂O: C, 52.10; H, 6.54; N, 13.00%. Found: C, 52.20; H, 6.64; N, 12.75%.

Measurements. UV–vis spectra were measured on JASCO V-570 or Shimadzu UV-2200 spectrophotometer. Circular dichroism spectra were obtained on JASCO J-720 spectropolarimeter. Transmission electron microscopy (TEM) was conducted on a Hitachi-H600 instrument by the negative staining method. 500 μ L of aqueous dispersions was mixed with 500 μ L of 2% aqueous uranyl acetate, and the mixture is applied to carbon-coated grids without ultrasonication. Infrared spectra were measured with a Shimadzu FTIR model DR-8000 (KBr pellet, resolution: 2 cm⁻¹) spectrometer. Water was purified by Milli-Q system. In the photoisomerization experiment of azobenzene unit, 500-W Hg lamp equipped with a Toshiba UV D35 filter was used as a light source.

Reconstitution Procedure. Stock solution of **4** (1 mM) was prepared by dissolving the sample in pure water or in ethanol/water mixture (1/1 by vol) by ultrasonication. Melamine derivatives were dissolved in ethanol (1 mM) and 100 μ L of the solution were injected in 2.9 mL of water or water–ethanol mixtures. Then, aqueous dispersion of **4** was added to the solution, and they were mixed by hand-shaking. In every case, time dependence of absorption and circular dichroism spectra after mixing was followed. Specimens for electron microscopy were prepared for dispersions in a stationary state. For spectral titration measurement, ethanolic solutions of melamine subunits were first injected into water, and then aqueous **4** stock solution was added to each solutions to give various melamine/cyanuric acid ratio, and the mixture were kept overnight before the measurement.

JA010035E